ELSEVIER

Polymer 41 (2000) 9163–9168

polymer

www.elsevier.nl/locate/polymer

Influence of segmental swelling of an asymmetric block copolymer on the morphology of melt-mixed immiscible polymer blends

J.R. Kim, S.D. Hudson, A.M. Jamieson*, I. Manas-Zloczower, H. Ishida

Department of Macromolecular Science and Engineering, Case Western Reserve University, Cleveland, OH 44106, USA

Received 28 January 2000; received in revised form 27 March 2000; accepted 5 April 2000

Abstract

We investigate the influence of an asymmetric PS-*b*-PMMA block copolymer (bcp) on the morphology of melt-mixed immiscible binary polymer blends containing poly(styrene-*co*-acrylonitrile) random copolymer (SAN) and poly(cyclohexylmethacrylate) (PCHMA). By varying the SAN copolymer composition, the balance between the swelling of each block segment located at the interface between the two phases is altered and the effect on blend morphology is studied. As in earlier studies using a symmetric bcp, we find that for a specified shear history, there is a zone of effective emulsification of the blend bounded by regions of internal and external emulsification failure. However, the locations of the boundaries between stable and unstable emulsification differ for an asymmetric versus a symmetric bcp. Thus the morphology depends not only on the segmental swelling ratio but also on the difference in the effective size of each bcp segment. Scaling arguments successfully correlate the limits of stable emulsification for both symmetric and asymmetric bcp.

Keywords: Block copolymer; Immiscible polymer blends; Segmental swelling

1. Introduction

The droplet size distribution of the minor component in immiscible polymer melt blends is determined by the processes of breakup and coalescence of droplets because of the shear and elongational forces exerted by the continuous phase during the mixing process. Droplet breakup produces smaller droplet sizes and droplet coalescence results in larger droplet sizes. Therefore, to obtain a more finely dispersed morphology, which generally enhances blend properties, it is necessary to enhance the breakup process and inhibit the coalescence of droplets.

The effect of a block copolymer (bcp) on the morphology of immiscible polymer blends in melt mixing has been studied theoretically [1–4] and experimentally [5–8], and it is concluded that the bcp can induce a finer morphology of an immiscible blend in two ways, viz.: (1) by decreasing the interfacial tension between each phase which results in smaller droplet size after breakup; and (2) by inhibiting coalescence of droplets due to the physical presence of the bcp at the interface between the two phases.

In previous work [7,8], we reported that the segmental swelling power ratio (σ_r) of the external block relative to the internal block of a bcp located at the surface of a droplet of the minor phase has an important effect on the morphology of an immiscible polymer blend. The segmental swelling power ratio, σ_r is [8–10]:

$$\sigma_r = \frac{S_{out}}{S_{in}} \tag{1}$$

where S_i is the segmental swelling power of block i, defined as the ratio of the block length in contact with the compatible blend component relative to the length in the neat copolymer. S_i was deduced by thermodynamic arguments [9,10] to be given by:

$$S = \frac{N}{P} - 2\chi N \tag{2}$$

with P, the degree of polymerization for the compatible blend component, N, the degree of polymerization for the compatible bcp segment and χ, the Flory–Huggins interaction parameter between the two. This expression is valid for $N \geq P$, i.e. under wet-brush conditions. S_{out} and S_{in} are the swelling powers for the bcp segments external and internal, respectively, to the droplets of minor phase. Specifically, we found that the morphology of a melt-mixed polymer blend of poly(styrene-*co*-acrylonitrile) random copolymer (SAN) and poly(cyclohexylmethacrylate) (PCHMA), compatibilized by a symmetric poly(methylmethacrylate-*b*-polystyrene)

* Corresponding author. Tel.: +1-216-368-4172; fax: +1-216-368-4202.
E-mail address: amj@po.cwru.edu (A.M. Jamieson).

0032-3861/00/$ - see front matter
PII: S0032-3861(00)00283-4

diblock copolymer (PMMA-*b*-PS; $N_{PMMA} \cong N_{PS}$), depends on the value of σ_r [8]. The morphology of the blends was examined after melt mixing under high shear, which is dominated by droplet breakup, followed by low shear, which exhibits droplet coalescence. When $\sigma_r > 2.5$, the morphology of the blend system shows external emulsification failure, in which very small micelles and large droplets coexist in the continuous phase; when $\sigma_r < 0.4$, the morphology of the blend shows internal emulsification failure, where small micelles reside inside large droplets of minor phase; when $2.5 > \sigma_r > 1.0$, the blend system is well emulsified and no coalescence is observed; when $1 > \sigma_r > 0.4$ the blend shows slow coalescence.

In this paper, we extend our earlier investigation to explore the influence of the swelling balance on the morphology of a melt-mixed blend containing an asymmetric bcp. Here, we expect that, in addition to the monomer interaction strength, the difference in chain length of each block will influence the emulsification behavior.

First, we note that our derivation of Eq. (2) considers the expansion of a polymer brush grafted onto a rigid wall. It was pointed out to us [11] that, in modeling a copolymer layer adsorbed to the interface between two immiscible polymers, this assumption precludes taking into account that the degree of swelling of each copolymer block is interdependent. The swelling power of one block in one polymer will be influenced by the swelling state of the other block with respect to the other polymer. This issue is especially important when the copolymer blocks are unequal in size. Wang and Safran [12] have calculated the equilibrium structure of such a copolymer layer. When the copolymer is swollen on both sides of the interface, the spontaneous curvature of the interface is proportional to (see Eq. (B3c) of Ref. [12]):

$$c_0 \sim (b_A^2 u_A N_A^2 - b_B^2 u_B N_B^2) \tag{3}$$

where b_i and u_i are, respectively, the Kuhn segment length and the second virial coefficient (excluded volume) of the i block. When the spontaneous curvature is zero, Eq. (3) indicates $b_A^2 u_A N_A^2 = b_B^2 u_B N_B^2$, and hence it is natural to define an asymmetry ratio:

$$\sigma_r = (b_A^2 u_A N_A^2 / b_B^2 u_B N_B^2) \tag{4}$$

For long-chain polymers in a shorter chain solvent of degree of polymerization P, and with Flory–Huggins interaction parameter χ, the second virial coefficient (the effective excluded volume for the long-chain segments) is

$$u = \nu(1/P - \chi) \tag{5}$$

where ν is a volume parameter roughly of the order of magnitude of the monomer volume. Thus we generalize Eq. (4) to

$$\sigma_r = [b_A^2 N_A^2 \nu_A (1/P_1 - \chi_1)]/[b_B^2 N_B^2 \nu_B (1/P_2 - \chi_2)] \tag{6}$$

In the present circumstance, we simplify Eq. (6) further by setting $b_A^2 \nu_A = b_B^2 \nu_B$, and hence obtain:

$$\sigma_r = [N_A^2 (1/P_1 - \chi_1)]/[N_B^2 (1/P_2 - \chi_2)] \tag{7}$$

It is interesting to note that, in the case of a symmetric bcp, this expression reduces to:

$$\sigma_r = [(1/P_1 - \chi_1)]/[(1/P_2 - \chi_2)] \tag{8}$$

which is fully consistent with our previous treatment [9,10] of the swelling balance based on Eq. (2). We may also note here a recent theoretical analysis by Frederickson and Bates [13] who derive an expression for the specific bcp composition, f_A, in asymmetric A/A-*b*-B/B blends at the isotropic Lifschitz point L, where the spontaneous interfacial curvature vanishes:

$$f_A = \frac{\sqrt{P_A/P_B}}{1 + \sqrt{P_A/P_B}} \tag{9}$$

Considering $f_A = N_A/N$, $1 - f_A = N_B/N$, the above relation can be rearranged into:

$$\frac{N_A^2}{N_B^2} \frac{P_B}{P_A} = 1 \tag{10}$$

which agrees with Eq. (7) above, i.e. when $\chi_1 = \chi_2 = 0$, a vanishing interfacial curvature requires $\sigma_r = N_A^2(1/P_1)]/[N_B^2(1/P_2)] = 1$ (see Eq. (3)).

Making contact with our previous work, we note that, to describe the asymmetry ratio of a bcp at the interface of a droplet of minor phase, Eq. (7) can be recast in the form:

$$\sigma_r = \frac{N_{out} S_{out}}{N_{in} S_{in}} \tag{11}$$

where N_{out} and N_{in} are the degrees of polymerization of the block segment external and internal to the droplet, and S_{out} and S_{in} are the corresponding segmental swelling factors, now defined in terms of the monomer excluded volume as $S_i = N_i u_i$, with $u_i = (1/P_i - \chi_i)$. Eq. (11) provides a simple scaling relation to delineate the limits of stable emulsification for both symmetric and asymmetric bcps, based on the requirement for approximately balancing the interfacial curvature.

2. Experimental

The blend components used in this study are a 218k PMMA-*b*-PS bcp (71k:147k; $M_w/M_n = 1.11$), obtained from Polymer Source Inc., PCHMA ($M_n = 38.5$k; $M_w/M_n = 3.47$) from Scientific Polymer Products Inc., and styrene–acrylonitrile copolymers (SAN) with 26 and 33% acrylonitrile content ($M_w = 153$k and 130k, and $M_w/M_n = 2.23$ and 1.95, respectively) supplied by Mitsui Toatsu Chemical Inc. The weight ratio of the major to minor component is 4:1 and 5% of bcp was added to the blend, without changing the ratio of major and minor components. The blend systems are designated major/minor/bcpa or

Table 1
Calculated values of Flory–Huggins parameter (χ), interfacial tension (Γ), and droplet size (D) for the uncompatibilized blends

	SAN26/PCHMA		SAN33/PCHMA		PCHMA/SAN26		PCHMA/SAN33	
$\dot{\gamma}$ (s^{-1})	50	1	50	1	20	1	20	1
η_m (Pa s)8	1420	7210	1340	6130	4260	12900	4260	12900
η_d (Pa s)	2910	12900	2910	12900	2080	7210	1920	6130
η_r	2.05	1.75	2.17	2.10	0.49	0.56	0.45	0.48
χ	0.0236	0.0236	0.0473	0.0473	0.0236	0.0236	0.0473	0.0473
Γ (mN/m)	1.73	1.73	2.44	2.44	1.73	1.73	2.44	2.44
D_{Taylor} (μm)	0.022	0.21	0.032	0.35	0.019	0.13	0.027	0.18
D_{Grace}	0.036	0.30	0.057	0.62	0.019	0.12	0.026	0.17
N_1 (kN/m^2)	250/470	8.3/17	15/470	4.8/17	470/250	17/8.3	470/150	17/4.8
D_{corr} (μm)	0.10	0.84	0.18	1.8	0.05	0.29	0.06	0.37
$D_{w,exp}$ (μm)	0.45	1.11	0.61	1.5	0.35	0.93	0.76	1.2

major/minor/bcp where bcp and bcpa indicate, respectively, symmetric and asymmetric bcp.

A Rheometrics RMS 800 rheometer was utilized for melt blending of the blend components to provide a well-specified simple shear deformation. A powder prepared by co-precipitation of bcp with the minor component was dry-mixed with the major phase, and then compression-molded at 200°C under vacuum to form discs. The disc-shaped specimens were sheared at 200°C in parallel plate geometry (7.9 mm diameter and 0.5 mm gap).

To observe the blend morphology, thin film sections were analysed using a RMC MT-7000 ultramicrotome, and a JEOL 100CX TEM, after staining with aqueous RuO_4 solution. The PS segment of the bcp and the SANs are stained with RuO_4 such that the PS segment is seen as the darkest regions, and the SAN phase is light gray. PCHMA is unstained by RuO_4. Therefore, microdomains of the bcp at the droplet interface or as micelles can be detected.

NIH image software was used to calculate the statistical sizes of the droplets from the TEM micrographs of the blends. The measured droplet sizes were converted to the weight average droplet size, which is defined as:

$$D_w = \Sigma(nD^4)/\Sigma(nD^3) \tag{12}$$

More details of the experimental procedures were as presented elsewhere [7,8].

3. Results and discussion

3.1. Uncompatibilized blends

For the uncompatibilized melt-mixed SAN*x*/PCHMA and PCHMA/SAN*x* blends, as thoroughly demonstrated in our previous studies [7,8], the droplets of minor phase break up into smaller droplets at high shear rate, and when the shear rate is subsequently stepped down to a low value, the small droplets coalesce into larger droplets. The coalescence of droplets is known to occur via droplet collision followed by drainage and rupture of the film between droplets [14,15]. The weight average droplet sizes analyzed by the image analysis software are shown in Table 1. The measured droplet sizes are larger than the theoretical droplet sizes calculated based on the Taylor equation [16]:

$$D = \frac{4\Gamma(\eta_r + 1)}{\dot{\gamma}\eta_m\left(\frac{19}{4}\eta_r + 4\right)} \qquad \text{when } \eta_r \le 4 \tag{13}$$

Here, D is the maximum stable diameter of the droplet, Γ is the interfacial tension, η_r is the relative viscosity, which is the ratio of the viscosity of droplet (η_d) to that of matrix (η_m) and $\dot{\gamma}$ is the shear rate. The Taylor equation is derived assuming each phase is a Newtonian fluid, and considering only breakup of a single droplet. Even for Newtonian liquids, Eq. (13) is found to be accurate only for viscosity ratios close to unity [17,18]. Based on experimental observation, Grace has proposed the following equation:

$$\log\left(\frac{\eta_m\dot{\gamma}D}{2\Gamma}\right) = -0.506 - 0.0994\log\eta_r + 0.124\log^2\eta_r - \frac{0.115}{\log\eta_r - \log\eta_{r,cr}} \tag{14}$$

which predicts slightly larger values, D_{Grace}, for our blends, also listed in Table 1, but still much smaller than those observed.

For a mixture of two non-Newtonian polymers, with a high concentration of minor phase (20%) as in our experiments, the Taylor equation is not expected to predict an accurate droplet size. The discrepancy between the predicted droplet size and the measured values may originate from the coalescence of droplets due to the high volume fraction of the minor component [6], or from the non-Newtonian characteristic and elasticity of the blend components [19]. Mighri et al. [19] recently investigated the influence of elasticity ratio (k_r) on breakup of droplets in simple shear. Here, the elasticity ratio is the ratio of the Maxwell relaxation time of the droplet (λ_d) to that of the matrix (λ_m) where the Maxwell relaxation time is defined as $\lambda = N_1/2\eta\dot{\gamma}^2$, and N_1 is the first normal stress difference. Mighri et al. [19] found that the droplet size increases with

increase of k_r when $k_r > 0.37$, and levels off at approximately 3.5 times the Taylor value when $k_r > 4$. An empirical correction was performed to the calculated droplet sizes based on the experimental results of Mighri et al. [19], using the measured normal stresses for each of the blend components (Table 1). The corrected droplet sizes, D_{corr}, are listed in Table 1, and are substantially closer but still smaller than the experimental data, particularly for the PCHMA/SAN*x* blends for which the matrix elasticity is higher than that of the droplet. The remaining discrepancy may be due to the effect of droplet coalescence [6].

3.2. Compatibilized blends

For the blend systems studied, the swelling factors, S_i, of each segment of the bcp are calculated using Eq. (12) and the interfacial asymmetry ratio, σ_r, is calculated from Eq. (13). The results are shown in Table 2. The morphologies of the SAN26/PCHMA/bcpa blend, sheared at a high rate followed by step down to a low rate, are shown in Fig. 1(a) and (b), respectively. Small droplets of minor PCHMA component are produced in the SAN matrix at high shear rate (Fig. 1(a)). When the low shear (1 s^{-1}) is applied for 20 min consecutively, the droplets show very little coalescence into larger droplets and remain predominantly as small droplets (Fig. 1(b)). This suggests that the droplets are well stabilized by the bcp located at the interface for which the asymmetry ratio $\sigma_r = 0.46$ (Table 1). However, the SAN33/PCHMA/bcpa blend system, which has a very small $\sigma_r = 0.05$, shows severe internal emulsification failure [2,3] as evidenced by the fact that micelles exist inside the minor phase droplets even at high shear rate

Table 2
Segmental swelling factors, S_i, and asymmetry ratios, σ_r, of blends containing a PS-*b*-PMMA block copolymer (bcpa)

Major/minor/bcp	S_{out}	S_{in}	S_{out}/S_{in}	N_{out}/N_{in}	σ_r
SAN26/PCHMA/bcpa	13.7	15.6	0.88	0.48	0.44
SAN33/PCHMA/bcpa	1.60	15.6	0.10	0.48	0.05
PCHMA/SAN26/bcpa	15.6	13.7	1.14	2.08	2.18
PCHMA/SAN33/bcpa	15.6	1.60	9.8	2.08	19.1

where more interfacial area is available for the bcp (Fig. 1(c) and (d)). The internal emulsification failure occurs because, when $N_{out}S_{out}/N_{in}S_{in}$ is very small the spontaneous interfacial curvature generated by the bcp segments is in the opposite direction (convex toward the minor phase) and much larger than that of the droplets formed by the mixing process.

For the PCHMA/SAN26/bcpa blend system, which has the inverse composition to SAN26/PCHMA/bcpa, the droplet size distribution is similar at high and low shear rates indicating little coalescence into larger droplets (Fig. 2(a) and (b)). There is no evidence of external or internal emulsification failure. This suggests that a stable curvature is formed by the bcp segments, which is consistent with the computed asymmetry parameter of the system ($\sigma_r = 2.18$). The morphology of the blend PCHMA/SAN33/bcpa, which has a very large asymmetry ratio ($\sigma_r = 19.1$), shows external emulsification failure, viz. at low shear, droplet coalescence occurs such that large droplets of minor phase coexist with small micelles in the continuous phase together with large minor phase droplets (Fig. 2(c) and (d)).

Thus, we find that, as for the symmetric bcp, the asymmetric bcp exhibits internal and external emulsification

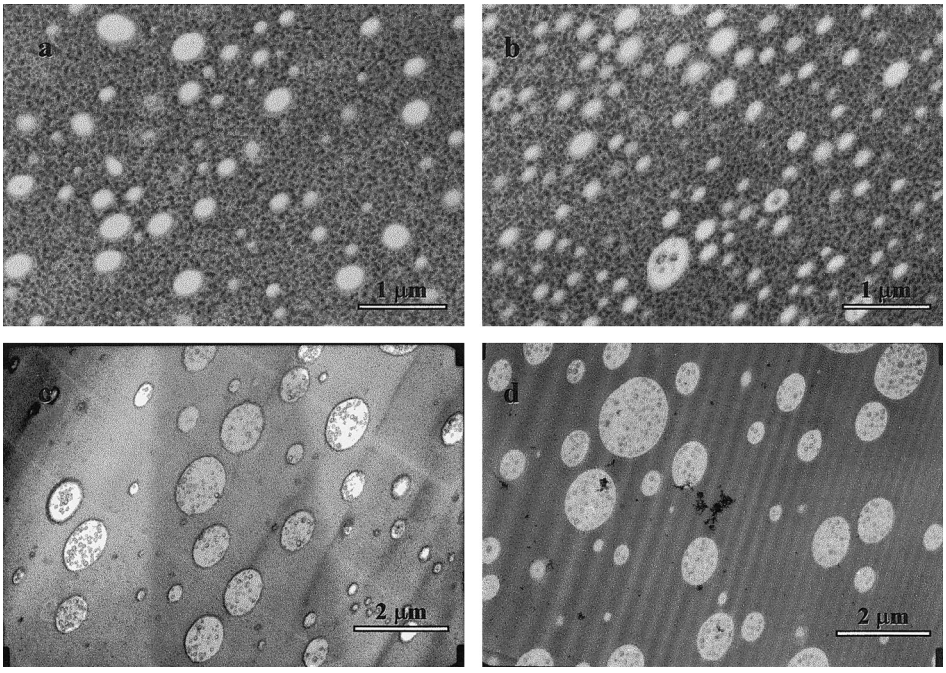

Fig. 1. The TEM micrographs of: (a) SAN26/PCHMA/bcpa sheared at 20 s^{-1} for 20 min; (b) SAN26/PCHMA/bcpa sheared at 1 s^{-1} after shearing at 20 s^{-1}, both for 20 min; (c) SAN33/PCHMA/bcpa sheared at 20 s^{-1} for 20 min; and (d) PCHMA/SAN33/bcpa sheared at 1 s^{-1} after shearing at 20 s^{-1}, both for 20 min.

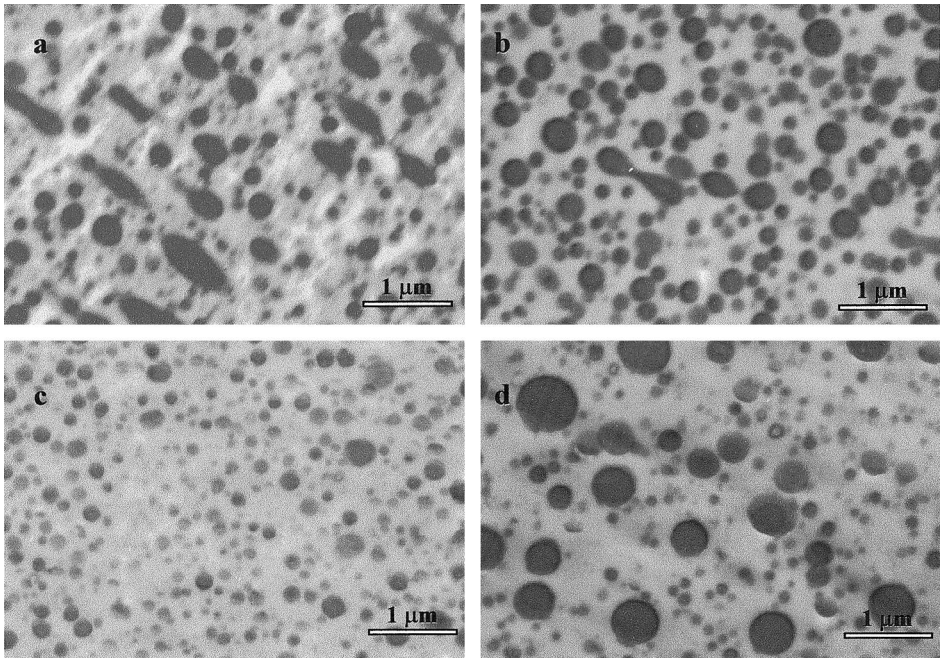

Fig. 2. The TEM micrographs of: (a) PCHMA/SAN26/bcpa sheared at 20 s^{-1} for 20 min; (b) PCHMA/SAN26/bcpa sheared at 1 s^{-1} after shearing at 20 s^{-1}, both for 20 min; (c) PCHMA/SAN33/bcpa sheared at 20 s^{-1} for 20 min; and (d) PCHMA/SAN33/bcpa sheared at 1 s^{-1} after shearing at 20 s^{-1}, both for 20 min.

failure, respectively, at very small and very large values of the interfacial asymmetry factor (Eq. (13)). When we superpose data for the present blend containing an asymmetric bcp with those earlier obtained [8] for blends containing a symmetric bcp on a plot of $S_{out}(N_{out}/N_{in})$ versus S_{in}, as shown in Fig. 3, we find that the boundaries delineating emulsification failure for the blends containing asymmetric bcp agree with those for the blend containing a symmetric bcp: viz. $\sigma_r < 0.4$, internal emulsification failure, $1 > \sigma_r > 0.4$, unstable emulsification, $2.5 > \sigma_r > 1$, stable emulsification, and $\sigma_r > 2.5$, external emulsification failure. It is interesting to point out that Leibler [2] found in the dry-brush limit ($S_i \sim 1$) that emulsification failure occurs for an asymmetric bcp when the ratio of block molecular weights is less than 0.45 or greater than 2.2, which seems quite consistent with our observation under wet-brush conditions that stable emulsification occurs when:

$$0.4 \leq \frac{N_{out}}{N_{in}} \frac{S_{out}}{S_{in}} \leq 2.5 \tag{15}$$

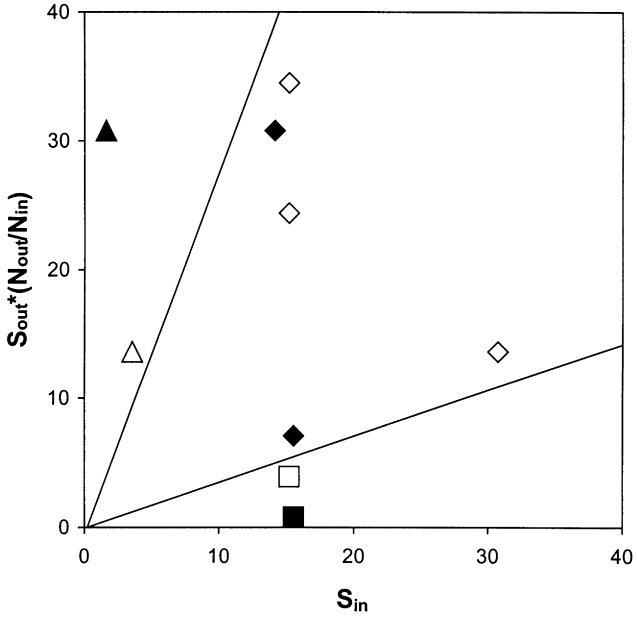

Fig. 3. The coalescence diagram based on the revised expression for the swelling power balance (Eq. (15)). Open symbols are from previous studies (Refs. [7,8]): S V, stable emulsion; K O, external emulsification failure; and A B, internal emulsification failure.

4. Conclusions

We have investigated the boundaries between effective emulsification and emulsification failure in melt mixing of immiscible polymer blends containing either an asymmetric or a symmetric bcp. Our observations for both classes of copolymer can be interpreted in terms of an interfacial asymmetry ratio derived from a theoretical treatment of the spontaneous interfacial curvature of a diblock copolymer film at the interface between immiscible monomeric liquids by Wang and Safran [12].

Acknowledgements

Financial support from the Edison Polymer Innovation Corporation, the General Electric Company, and NSF Grant CTS-9731502 is gratefully acknowledged. We are

also indebted to Prof Zhen-Gang Wang of the California Institute of Technology, who provided the theoretical arguments leading to the definition of the interfacial asymmetry parameter (Eq. (4)).

References

[1] Noolandi J, Hong KM. Macromolecules 1982;15:482.
[2] Leibler L. Macromol Symp 1988;16:1.
[3] Wang ZG, Safran SA. J Phys (Paris) 1990;51:185.
[4] Milner ST, Xi H. J Rheol 1996;40:663.
[5] Fayt R, Jerome R, Teyssie Ph. Makromol Chem 1986;187:837.
[6] Sundararaj U, Macosko CW. Macromolecules 1995;28:2647.
[7] Kim JR, Jamieson AM, Hudson SD, Manas-Zloczower I, Ishida H. Macromolecules 1998;31:5383.
[8] Kim JR, Jamieson AM, Hudson SD, Manas-Zloczower I, Ishida H. Macromolecules 1999;32:4582.
[9] Braun H, Rudolf B, Cantow HJ. Polym Bull 1994;32:241.
[10] Adedeji A, Hudson SD, Jamieson AM. Polymer 1997;38:737.
[11] Wang Z-G. Private communication, 2000.
[12] Wang Z-G, Safran SA. J Chem Phys 1991;94:679.
[13] Frederickson GH, Bates FS. J Polym Sci Polym Phys 1997;35:2775.
[14] Chesters AK. Trans Inst Chem Eng 1991;69A:259.
[15] Ramic AJ, Hudson SD, Jamieson AM, Manas-Zloczower I. Macromolecules 2000;33:371.
[16] Taylor GI. Proc R Soc London, A 1934;146:501.
[17] Grace HP. Chem Eng Commun 1982;14:225.
[18] Ramic AJ, Hudson SD, Jamieson AM, Manas-Zloczower I. Polymer 2000;41:6263.
[19] Mighri F, Carreau PJ, Ajji A. J Rheol 1998;42:1447.